SEISMIC DETECTABILITY OF AVALANCHES ON MARS Antoine Lucas[1], Saksham Rohilla[1], Anne Mangeney[1], Lucas Bourdon[1], Gregory Sainton[1], Chahana Nagesh[1], Taichi Kawamura[1], Clément Perrin[1], Sebastien Rodriguez[1], Philippe Lognonné[1], [1]Université Paris Cité, Institut de physique du globe de Paris, CNRS, Paris, France (lucas@ipgp.fr).

Motivation: Like on the Earth, mass wasting such as granular (i.e., rock, dust as well as snow/ice) avalanches are known to be active on Mars [1, 2]. Their dynamics has a few implications in terms of climatic conditions and triggering mechanisms. Notwithstanding, their dynamics is yet to be understood. In generally, previous studies have been based on interpretations of the geomorphic features by comparison with known processes occurring on Earth and/or with experimental works as well as numerical simulations [e.g., 3–9]. Anyhow, all of these approaches remain limited in terms of ability of constraining the avalanche dynamics.

As a matter of fact, if the imaging and in particular, the high resolution one allowed to make great advances in the morphological characterization of the deposits, and that the analogical and numerical simulations brought constraints, it does not remain about it that we miss today insights on their dynamics [7]. As a matter of fact, many authors have proposed dry dispersion of fine dust or wet processes [e.g., 10, 11]. For example, [12] proposed discharge from a saline groundwater spring.

On the other hand, seismology offers a unique path to the force history assessment [e.g., 13, 14]. The InSight mission has delivered almost 2 Martian years of seismic recording. Many events have been detected and only some of them have been properly identified as marsquake, impact or atmospheric turbulence etc.[e.g., 15]. To date, none of these signals have been attributed to avalanches [16], but we are discussing the conditions necessary for such a detection to be possible.

Methods: Thanks to the orbital imagery (mainly from both CTX and HiRISE data), we investigate several areas around the InSight landing site (135.61°E 4.49°N) in order to evaluate the mass wasting formation rates and offset distances from the SEIS seismometer. The resulting mapping is given in Fig. 1. We identified two main clusters: the first being in a 300 km range from SEIS, mainly composed of rock avalanches and gullies' like. The second group, mainly composed of dust avalanches (i.e., slope streaks), is located further east, at a distance of about 1000 km away from the seismometer.

The data collection is being used to characterize the typical values for the geomorphic metrics of the avalanches (i.e., volume, runout, thickness). We also derived digital elevation models from the imagery, that we combined with large scale elevation grids from both MOLA and HRSC in order to constrain the topographical profiles along with the avalanches occurred.
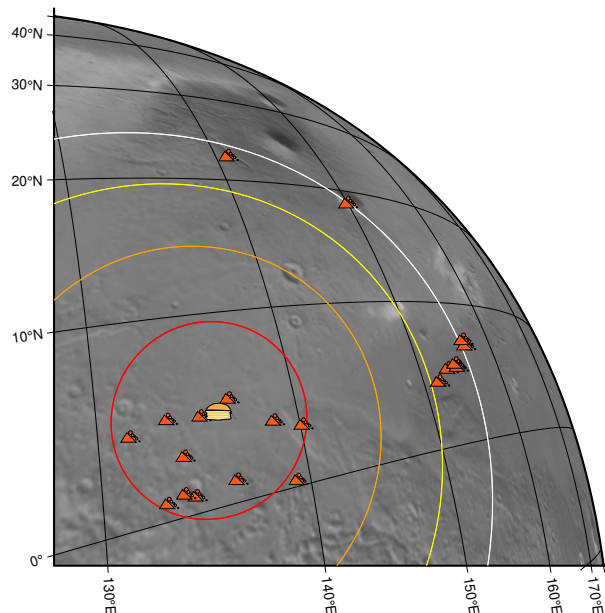

Figure 1: Identified avalanches around the InSight landing site (135.61°E 4.49°N). Circles correspond to a distance $\Delta = \{5°, 10°, 15°, 20°\}$, from red to white respectively to the SEIS instrument.

Hence, we can estimate the force drop on the ground during the avalanche motion, which is very close to a sinusoidal source [13, 17]. Its amplitude F_p scales with $\mu M g$, μ being the apparent friction (i.e., ratio of the shear force to the normal force), M the mass and g the acceleration due to gravity (Fig. 2). Its duration τ can be estimated from analytical solution [see supp. of 7]. We end up with the broadband signal and high frequency content (mainly due to impact, collision and fracturing) is not accounted for at this stage. Such simplistic synthetic force-time function have been compared and validated with more complex force fields obtained after numerical simulations [13, 16]. The over simplification model also assumes mass conservation and hence no volume variation during the emplacement phase.

The Green's functions are obtained from the IRIS Synthetics Engine webservice Syngine [18], which provides on demand custom 3D AxiSEM synthetic seismograms based on both terrestrial and martian models [19, 20]. Using our synthetic force-time function with the Green's functions, we end up with synthetic seismograms associated to avalanches.
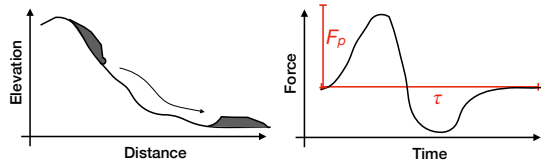
Figure 2: Idealized avalanche source time function for the vertical component, inspired from [17].

Finally, we extracted typical ambient signal (i.e., noise) form the data in order to evaluate the detectability of the events considering epicentral distance, frictional parameters and mass volumes of the {rock/dust/snow} avalanches.

Results and discussion: First, we demonstrate the validity of our approach by comparing with an actual rock avalanche event on Earth (Fig. 3-a). Then, we show that the detectability conditions on Mars differ from the Earth. First, the ambient noise on both planets is very different (in particular below 1 Hz), mainly due to the absence of ocean and a very different atmosphere contribution on Mars [15, 20] (Fig. 3-b).
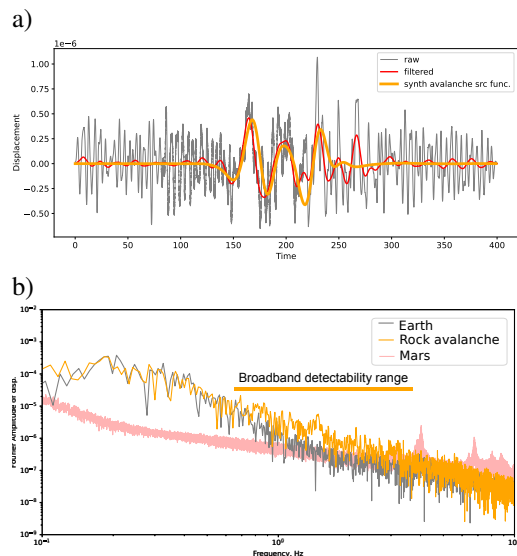
a)

b)

Figure 3: a) Comparison between the synthetics and actual rock avalanche event on Earth. b) Example of the ambient noise on Earth (gray) and Mars (red) with an unfiltered seismic signal of the rock avalanche above. Its terrestrial broadband detectability range is highlighted by the orange box.

For a given force applied to the ground (i.e., which would correspond to a different avalanche on Mars, as gravity will affect the weight and the resulting friction force) the amplitude of the resulting seismic signal is higher on Mars. For example, if F_p = 4.5 10^9 N, with

τ = 100 s (which would correspond to a typical 10^6 m^3 rock avalanche on Earth), and for a given epicentral distance, the amplitude of the resulting seismic signal in displacement is almost 2 times higher on Mars (Fig. 4). Consequently, for a given volume, this almost compensates the smaller weight due to a small acceleration due to gravity as the maximum amplitude of the avalanche induced seismic signal scales with the point source maximum amplitude F_p for a given topographic profile. On a more subtle level, the friction coefficient is also affecting this scaling as well.
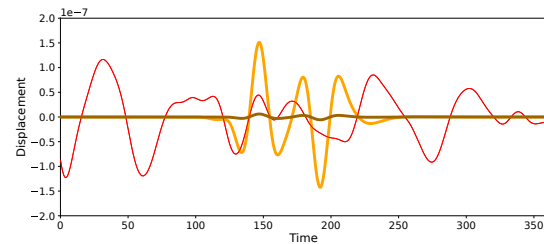

Figure 4: Synthetic seismic signal induced by theoretical avalanche source time function accounting for Mars model. Thick orange curve is an avalanche with a volume V of 2.10^6m^3, and brown is for V = 200k m^3, both at 52 km. Thin red curve is a filtered SEIS record in abscence of identified event.

We find that large volumes ($>$ Mm^3) can be detected up to $\Delta \simeq 3$ degrees. Smaller dust avalanches with a typical volume of 200 km^3 are barely detectable at larger distances of 50 km, depending on the considered models and seismic activity. Investigation on second order parameters are on going.

References: [1] N. Schorghofer et al., *Icarus* **2007**. [2] P. Russell et al., *Geophy. Res. Let.* **2008**. [3] G. S. Collins, H. J. Melosh, *J. Geophys. Res.* **2003**. [4] M. F. Gerstell et al., *Icarus* **2004**. [5] H. Miyamoto, *Journal of Geophysical Research* **2004**. [6] D. Baratoux et al., *Icarus* **2006**. [7] A. Lucas et al., *Nature Comm.* **2014**. [8] C. M. Dundas, *Nature Geoscience* **2020**. [9] A. Valantinas et al., *Planetary and Space Science* **2021**. [10] N. Schorghofer et al., *Geophys. Res. Lett.* **2002**. [11] C. B. Phillips et al., *Geophysical Research Letters* **2007**. [12] J. W. Head et al., *Lunar and Planetary Science Conference* **2007**. [13] P. Favreau et al., *Geophys. Res. Lett.* **2010**. [14] L. Toney, K. E. Allstadt, *Seismological Research Letters* **2021**. [15] D. Giardini et al., *Nature geoscience* **2020**. [16] A. Lucas et al. in 51st Lunar and Planetary Science Conference, **2020**, Abstract #1840. [17] E. Brodsky et al., *Geophysical Research Letters* **2003**. [18] IRIS DMC, Data Services Products: Synthetics Engine, **2015**. [19] T. Nissen-Meyer et al., *Solid Earth* **2014**. [20] S. Stähler et al., *IPGP Data Center* **2021**.